(18) (a) F. Zingales, U. Satorelli, and A. Trovati, *Inorg. Chem.*, **6**, 1246 (1967); (b) F. Zingales, M. Graziani, F. Faraone, and U. Belluco, *Inorg. Chim. Acta*, 1, 172 (1967); (c) I. Wender and P. Pino, Eds., "Organic Synthesis via Metal Carbonyls", Vol. 1, Interscience, New York, 1968, pp 231–232; (d) M. S. Wrighton, D. L. Morse, and L. Pdungsap, *J. Am. Chem. Soc.*, **97**, 2073 (1975).
(19) P. J. Giordano and M. S. Wrighton, *Inorg. Chem.*, **16**, 160 (1977).
(20) M. S. Wrighton and D. L. Morse, *J. Organomet. Chem.*, **97**, 405 (1975).
(21) (a) M. S. Wrighton, H. B. Abrahamson, and D. L. Morse, *J. Am. Chem. Soc.*, **98**, 4105 (1976); (b) H. B. Abrahamson and M. S. Wrighton, *Inorg. Chem.*, 17, 3385 (1978).
(22) H. Saito, J. Fujita, and K. Saito, *Bull. Chem. Soc. Jpn.*, **41**, 359, 863 (1968).
(23) B. J. Tabner and J. R. Yandle, *J. Chem. Soc. A*, 381 (1968).
(24) (a) M. S. Wrighton, D. L. Morse, H. B. Gray, and D. K. Ottesen, *J. Am. Chem. Soc.*, **98**, 1111 (1976); (b) R. A. N. McLean, *J. Chem. Soc., Dalton Trans.*, 1568 (1974).
(25) N. J. Turro, "Molecular Photochemistry", W. A. Benjamin, New York, 1967.
(26) M. S. Wrighton, L. Pdungsap, and D. L. Morse, *J. Phys. Chem.*, **79**, 66 (1975).
(27) M. S. Wrighton, D. I. Handeli, and D. L. Morse, *Inorg. Chem.*, **15**, 434 (1976).
(28) (a) J. Kordas and M. A. El-Bayoumi, *J. Am. Chem. Soc.*, **96**, 3043 (1974); (b) M. A. El-Bayoumi and F. M. A. Halim, *J. Chem. Phys.*, **48**, 2536 (1968); (c) H. Stegemeyer, *Ber. Bunsenges. Phys. Chem.*, **72**, 335 (1968); (d) R. J. Watts and D. Missimer, *J. Am. Chem. Soc.*, **100**, 5350 (1978).
(29) (a) H. Taube, *Surv. Prog. Chem.*, **6**, 1 (1973); (b) P. C. Ford, *Coord. Chem. Rev.*, **5**, 75 (1970); (c) T. Matsubara and C. Creutz, *J. Am. Chem. Soc.*, **100**, 6255 (1978), and references cited therein.
(30) J. Saltiel, J. D'Agostino, E. D. Megarity, L. Metts, K. R. Neuberger, M. S. Wrighton, and O. C. Zafiriou, *Org. Photochem.*, **3**, 1 (1973).
(31) G. A. Crosby, K. W. Hipps, and W. H. Elfring, Jr., *J. Am. Chem. Soc.*, **96**, 629 (1974).
(32) $pK_a^* = pK_a^0 + (2.86\Delta\nu/2.3RT)$ where pK_a^0 is the overall acid dissociation constant for the ground state and $\Delta\nu$ is in cm^{-1} measured from the difference in absorbtion maxima. R and T have their usual meanings.
(33) J. F. Ireland and P. A. H. Wyatt, *Adv. Phys. Org. Chem.*, **12**, 131 (1976).
(34) W. H. Melhuish, *J. Opt. Soc. Am.*, **52**, 1256 (1962).
(35) J. G. Calvert and J. N. Pitts, Jr., "Photochemistry", Wiley, New York, 1966, p 799.
(36) J. N. Demas and G. A. Crosby, *J. Phys. Chem.*, **75**, 991 (1971).

Quantitative Studies of Chemical Reactivity of Tetra-μ-butyrato-dirhodium(II) Complexes

Russell S. Drago,* S. Peter Tanner,* Robert M. Richman, and John R. Long

Contribution from the School of Chemical Science, University of Illinois, Urbana, Illinois 61801, and the University of West Florida, Pensacola, Florida 32504.
Received August 28, 1978

Abstract: We have studied the thermodynamics of adduct formation for 1:1 and 2:1 adducts formed by Lewis bases with $Rh_2(C_4H_7O_2)_4$ in benzene solutions. Electrochemical studies of these adducts were also carried out in CH_2Cl_2. Corrections for a benzene–acid interaction were necessary to obtain solvent minimized enthalpies of acid–base adduct formation. The thermodynamic data clearly demonstrates substantial changes in the acidic and redox properties of the second metal as a result of base coordination to the first. The metal–metal bonding in the system causes this dimer to be a most unusual Lewis acid, as evidenced by deviations of the E and C predicted enthalpies from those observed. The unusual Lewis acid properties are attributed to the enhanced π-back-bonding capability of the rhodium(II) center as a result of extensive mixing of orbitals with π symmetry on the two metal centers. This causes the rhodium(II) center to be very effective in π-back-bonding to the axial ligands. The reduction potentials of $Rh_2(C_4H_7O_2)^+$, $Rh_2(C_4H_7O_2)_4B^+$, and $Rh_2(C_4H_7O_2)_4B_2^+$ are analyzed, and provide further support for the extensive π-back-bonding capabilities of this metal cluster.

Introduction

In recent years, considerable interest has been generated in the area of metal cluster chemistry. Clusters are found in a variety of important biological systems such as the ferredoxins,[1] nitrogenase,[1] cytochrome oxidase, and copper type 3 proteins.[2] In both heterogeneous and homogeneous catalytic systems, metal clusters are reported to effect some intriguing, industrially important reactions. Different mechanisms have been suggested to account for the synergistic ways in which one metal can influence the chemistry at a second metal site.[3]

In various systems, considerable variation exists in the extent of metal–metal interaction. In some, strong metal–metal bonds exist;[4] in others, the metals are interacting in a magnetic sense, but a direct metal–metal bond is absent; in still others, the metals are far enough removed to be noninteracting even in a magnetic sense. A continuum of systems exists which spans the classifications given above. Thus, there are a very large number of variables that can influence a very large number of different synergistic reaction mechanisms. A more complete understanding of this area leading to a full appreciation of the potential of metallomers for novel reaction types will require extensive investigation of many different types of systems. In addition to structural investigations, quantitative studies of chemical reactivity (kinetic and thermodynamic) must be carried out to determine ways and extents to which a second, third, etc., metal atom in a molecule can influence the coordination chemistry and redox chemistry at the first metal site.

Our initial selection of a system for investigation involved the dimeric metal carboxylates because of the extensive structural information available on them.[5] For stability reasons and because of the interest in the metal in catalytic systems, dimeric rhodium(II) acetate was selected. Its synthesis was reported[6] in 1963, and adducts with Lewis bases having both 1:1 and 2:1 stoichiometries were isolated. The crystal structure of the diaquo adduct[5] showed that this complex is isostructural with copper acetate, with each rhodium bound to one oxygen of each of the four acetate groups. The water molecules were found to lie along the fourfold axis defined by the rhodium–rhodium bond. The published metal–metal separation is 2.3855 Å. The analogous butyrate system is illustrated in Figure 1. Kitchens and Bear isolated 1:1 dimethyl sulfoxide and dimethyl sulfide base adducts of rhodium(II) acetate by thermally generating them from the 2:1 adducts.[7]

Molecular orbital calculations of various[8-10] types have been carried out to aid in the elucidation of the electronic structure of the metal dimers. A self-consistent charge and configuration molecular orbital calculation predicted a net single bond between the rhodium atoms.[9] More recently, Norman and Kolari have performed SCF-Xα scattered wave calculations on the diaquo adduct of rhodium(II) acetate.[10] They found a net bond

0002-7863/79/1501-2897$01.00/0

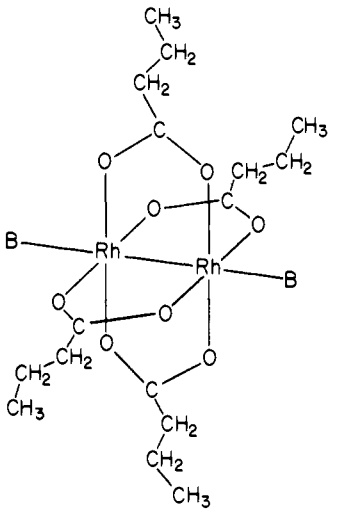

Figure 1. Schematic structure of 2:1 adducts of rhodium butyrate with a base B.

order of one and assigned the lowest energy electronic transition as $\pi^* \rightarrow \sigma^*$. The essential features of the metal–metal interaction are identical with those proposed earlier in a qualitative molecular orbital diagram used to interpret the EPR spectra of a nitroxide adduct of the rhodium(II) trifluoroacetate dimer.[11]

Wilson and Taube have shown that common oxidizing agents react with rhodium(II) acetate to form a new species.[12] Potentiometric and spectrophotometric titrations indicated that 1 equiv of oxidizing agent was consumed per mol of dimer. An Evans method susceptibility determination indicated that the resulting species has one unpaired electron per dimer.

In any fundamental study of the coordination process in which one is investigating the possible existence of unusual effects, it becomes essential to establish what is usual. An empirical, four-parameter equation has been reported to describe bond strengths of adducts in which the interaction involves σ bond formation. The enthalpy of interaction measured in a poorly basic, nonpolar solvent can be predicted for the "usual case" with

$$-\Delta H = E_A E_B + C_A C_B \qquad (1)$$

where ΔH is the enthalpy of adduct formation, subscripts A and B represent the Lewis acid and base, and E and C roughly parallel the qualitative assignment of tendencies of acids and bases to undergo electrostatic and covalent interaction. It has been shown previously[13] that the existence of extra effects (e.g., π-back-bonding or steric effects) in the coordination process can be demonstrated by first empirically determining the acid (or base) parameters on systems where the effect cannot exist. If the extra effect exists in the suspected system, the measured enthalpy will deviate from that predicted with eq 1. Seven bases with known E_B and C_B parameters[13] have been chosen for study with the rhodium dimer in order to determine via the E and C model whether or not the metal–metal bond gives rise to any unusual effects in the coordination chemistry of these systems.

Even though few previous studies have been reported for rhodium(II) butyrate, it was selected for the studies reported herein since it provides an almost ideal system for a quantitative determination of coordinate bond strengths. It has an obvious structural similarity to the characterized acetate, but has superior solubility properties to the acetate in nonpolar, very weakly basic solvents. With many bases, rhodium butyrate forms extensive amounts of a 1:1 adduct before coordination of the second base becomes significant (as determined from isosbestic points in the absorption spectra). This facilitates an otherwise often nearly impossible problem of spectroscopically determining accurate thermodynamic data for both steps in the reaction.[14]

Experimental Section

A. Preparations and Purification. Rhodium acetate[15] was prepared by literature methods. Conversion to the butyrate was effected by exchange with butyric acid. A similar exchange reaction has been reported for the preparation of molybdenum trifluoroacetate.[16] Rhodium acetate (1.3 g) was refluxed in butyric acid (30 mL) for about 3 h. The solvent was removed under vacuum. The solid product was extracted with hot benzene, filtered, and concentrated to 150 mL. Green rhodium(II) butyrate crystallized out of the cooled solution. The product was obtained by filtration and heated under vacuum at about 150 °C to remove excess butyric acid. Satisfactory carbon and hydrogen analyses were obtained.

A solution (1 mL) of 0.0160 g (2.89×10^{-5} mol) of rhodium butyrate and pyridine (5.78×10^{-5} mol) in benzene was used for a molecular weight determination. A value of 707 was obtained compared to a molecular weight for the 2:1 adduct of 712.

All bases used were purified by literature methods[17] and stored in a desiccator over magnesium perchlorate. Benzene solutions of the bases were used for both calorimetry and in the preparation of solutions for measurement of spectra. Benzene was dried over molecular sieves. Solutions were prepared immediately before use. Solutions of caged phosphite and 4-methylpyridine N-oxide were prepared in a glovebag under dry nitrogen.

B. Calorimetry. The calorimeter and the procedure for its use have been described.[18] Owing to limited solubility, the concentration of rhodium butyrate in benzene was limited to about 2.5×10^{-3} M. Solutions were prepared by dissolving weighed amounts (~0.08 g) of rhodium butyrate in about 40 mL of warm benzene (70 °C). The solution was quickly cooled to room temperature, brought to 50.0 mL in a volumetric flask, and then transferred to the calorimeter using 5 mL (or 3 mL) of benzene as a rinse. The calorimeter and solutions were then allowed to equilibrate for about 15 min before heat measurements were made. Though the solutions were supersaturated with rhodium butyrate at room temperature, the complex did not precipitate out of solution during the equilibration period. Since all the 1:1 and 2:1 adducts are soluble, precipitation was thus avoided during the calorimetry measurements.

The cumulative amount of heat evolved, H', resulting from sequential additions of base, has additive contributions from the two species formed. Using K_1 and K_2 from the spectral studies, the concentrations of 1:1 and 2:1 adducts are calculated for each initial base and initial acid concentration. All measured H' values are used with the known solution volumes, V, to set up a series of simultaneous equations of the form

$$H' = ([1:1]\Delta H^\circ_{1:1} + [2:1](\Delta H^\circ_{1:1} + \Delta H^\circ_{2:1}))V \qquad (2)$$

These equations are used to solve for the two unknowns, $\Delta H^\circ_{1:1}$ and $\Delta H^\circ_{2:1}$. The calorimetric and spectrophotometric results used to evaluate the thermodynamic data reported in this article are presented in the microfilm edition of this journal.

C. Cyclic Voltammetry. Cyclic voltammetry studies were conducted using a PAR Model 173 potentiostat/galvanostat and Model 176 current-to-voltage converter and recorded on a Tektronix 564 storage oscilloscope. Steady-state voltammograms were obtained by allowing the potential to cycle several times at each scan rate. The reference electrode was a silver wire suspended in a saturated AgI solution of CH_2Cl_2 which was 0.05 M in Bu_4NI and 0.42 M in Bu_4NBF_4.[19] Electrolyte solutions were 0.42 M Bu_4NBF_4 in CH_2Cl_2. (Nitromethane and other more polar solvents as well as ClO_4^- and PF_6^- anions changed the color of rhodium butyrate solutions, presumably owing to adduct formation, and were therefore unsatisfactory.) Rhodium butyrate solutions were 2.5×10^{-3} M; 3.0 mL was used per run.

The standard three-electrode arrangement was used. Because the potentials employed would oxidize mercury, platinum wire was used for the working and auxiliary electrodes. Following Adams,[20] the electrodes were cleaned before each run by immersion in dichromate–sulfuric acid to remove organic films and oxidize the surface, rinsed with distilled water and acetone, dried at 90°C, then electrolyzed at 0.0 V or less vs. Ag^+/Ag to reduce the surface to Pt(0).

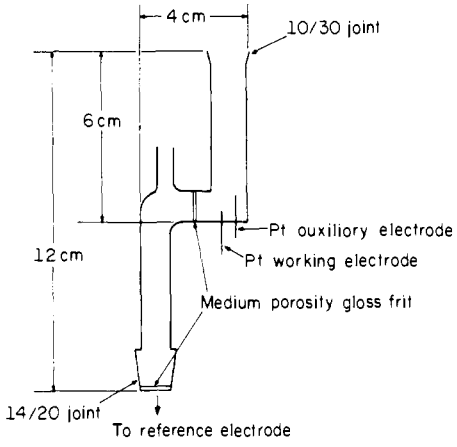

Figure 2. Cell designed for cyclic voltammetry. The volume of the working compartment is ca. 3 mL and that of the bridge is ca. 4 mL.

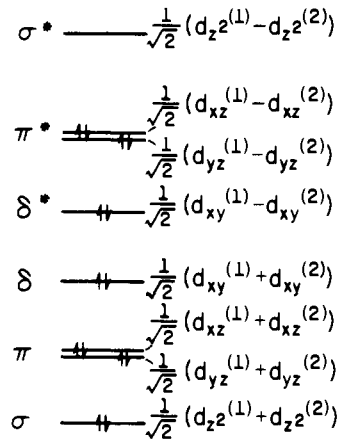

Figure 3. Qualitative MO diagram of rhodium butyrate showing combinations of metal 4d orbitals only.

Because of the special nature of these experiments, it was deemed necessary to design a new cell. The considerations were as follows: (1) owing to the high cost of rhodium, the working compartment should be as small as possible; (2) to reduce both Faradaic and non-Faradaic currents, the working electrode should be as small as is feasible; (3) to minimize the cell resistance, the distance between working and reference electrodes (controlled by the size of the bridge) should be kept small. The cell design that best met these criteria is illustrated in Figure 2. It was used in all the experiments described in this section. Note that, in addition to meeting the above requirements, this cell is suitable for use with air-sensitive compounds, since the working compartment is closed to the atmosphere.

Results and Discussion

A. Electronic Structure of Rhodium(II) Butyrate and Its Adducts. In a study of a nitroxide free radical adduct of the rhodium trifluoroacetate dimer in this laboratory,[11] a molecular orbital diagram with intuitive appeal to chemists was reported for rhodium carboxylate dimers. The relative molecular orbital energies were derived from perturbation-type considerations and are illustrated in Figure 3. The d orbital manifold is uninterrupted by ligand orbitals, the major metal–ligand interaction involves the σ-bonding oxygen orbital pushing up $d_{x^2-y^2}$, and the remaining splitting is proportional to the overlap of similar orbitals from the two metal centers. Hence, with the rhodium–rhodium bond defining the z axis, the neighboring d_{z^2} orbitals can overlap to form σ-bonding and antibonding combinations. Similarly, d_{xz} orbitals on the two centers overlap a little less to form π and π^* MOs. The d_{yz} orbitals form symmetry-equivalent π and π^* MOs, while the d_{xy} orbitals can have a small but finite overlap to form δ and δ^* MOs. While two of the published molecular orbital calculations[8,9] differ with this qualitative scheme in some respects, the very recent SCF-Xα calculation by Norman and Kolari[10] verifies all the essential features. This qualitative scheme has the advantage of providing a simple but reasonably accurate picture of the nature of these MOs.

The dimer can function as a Lewis acid by accepting electron density from one or two Lewis bases in the antibonding σ^* molecular orbital. This interaction raises the energy of both the σ and σ^* levels with adduct stability arising largely from the stabilization of the essentially donor lone-pair orbitals. The 1:1 adduct is thus a three-center type of bonding interaction and the 2:1 adduct a four-center type of bond. No quantitative characterization of the reactivity of a four-center system has been reported and the three-center system is unique in that one of the terminal atoms is a metal. Accordingly, it is of interest to obtain quantitative information on the coordination tendencies of these Lewis acid centers.

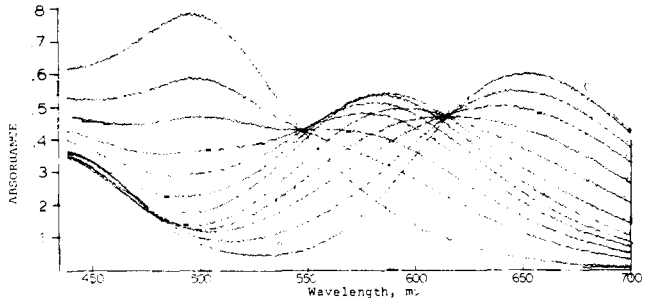

Figure 4. Spectrophotometric titration of rhodium(II) butyrate (2.439×10^{-3} M) with Me_2SO. The vertical lines indicate the wavelengths selected for analysis. The free acid spectrum is laeled with a "0".

B. Calorimetric and Spectrophotometric Data. The addition of Lewis bases to benzene solutions of the rhodium dimer causes pronounced spectral changes as illustrated in Figure 4 for the base dimethyl sulfoxide. As the mole ratio of base to rhodium dimer increases, one first observes isosbestic behavior for the free acid and 1:1 adduct at 616 nm followed by isosbestic behavior for 1:1 and 2:1 adducts at 547 nm. Equilibrium constants at room temperature were evaluated from a best fit of the absorbance data at four wavelengths. The number of unknowns can be minimized by selecting the isosbestic wavelengths as two of the four. At the 1:1 isosbestic point, for example, ϵ_F (the extinction coefficient for the free acid) is known and equals $\epsilon_{1:1}$. At this wavelength, information about the 1:1 to 2:1 equilibrium can be obtained from absorbance data in the more concentrated base solutions. The values obtained are reported in Table 1, and the raw absorbance data are presented in the microfilm edition.

Calorimetric measurements were carried out at room temperature. The heat evolved, H', as a function of base concentration is reported in the microfilm edition. The spectrophotometrically determined equilibrium constants were used to calculate the concentration of the 1:1 and 2:1 adducts. These values were substituted into eq 2 and the best fit values of $\Delta H°_{1:1}$ and $\Delta H°_{2:1}$ were determined and reported in Table 1. Error limits on ΔH were obtained by employing K values at the extreme of their respective error limits and redetermining the fit of the enthalpy data.

There are several interesting aspects to the data in Table 1. The equilibrium constants for binding indicate a greatly decreased acceptor capability for coordination of the second base relative to the first. Statistical considerations for noninteracting metal centers would lead to $K_1 = 4K_2$ if the metal centers were uncoupled. The observed ratio of K_1 to K_2 is much greater, as

Table I. Thermodynamic Data for Forming 1:1 and 2:1 Base Adducts of Dimeric Rhodium(II) Butyrate in Benzene Solution[a]

base	K_1	K_2	$-\Delta H_{1:1}$, kcal mol^{-1}	$-\Delta H_{2:1}$, kcal mol^{-1}
CH_3CN	$1.7 \pm 0.2 \times 10^3$	27.0 ± 2	5.1 ± 0.2	8.3 ± 0.4
C_5H_5N	$1.6 \pm 0.2 \times 10^8$	$2.4 \pm 0.2 \times 10^4$	11.2 ± 0.2	11.2 ± 0.3
N-Melm[b]	$\sim 10^9$	$8 \pm 13 \times 10^4$	12.4 ± 0.3	10.5 ± 0.5
piperidine[b]	$\sim 10^9$	$6 \pm 4 \times 10^4$	13.2 ± 0.1	12.5 ± 0.4
$[-CH_2CH_2]_2S$	$1.7 \pm 0.1 \times 10^7$	$1.9 \pm 0.3 \times 10^4$	11.0 ± 0.3	10.3 ± 0.4
caged phos	$9.1 \pm 0.7 \times 10^7$	$2.6 \pm 0.1 \times 10^4$	12.9 ± 0.2	11.3 ± 0.2
4-Pic-NO	$2.4 \pm 0.3 \times 10^5$	$2.9 \pm 0.3 \times 10^2$	5.0 ± 0.2	6.4 ± 1.4
$(CH_3)_2SO$	$1.1 \pm 1 \times 10^5$	$5.5 \pm 0.3 \times 10^2$	6.6 ± 0.2	6.5 ± 0.4

[a] The influence of errors in K on the ΔH's was checked by varying both K_1 and K_2 by two marginal standard deviations. The larger error obtained by either this procedure or the calorimetric data fit is reported as the error limit. For piperidine and 1-methylimidazole the latter error was used. [b] ΔH's calculated from calorimetric data by fixing K_1 at 1×10^9 and fitting ΔH_1, ΔH_2, and K_2. The values obtained are not changed within experimental error by variations of the fixed value of K_1 by 10^2.

Table II. Solvation-Corrected Enthalpies

base	$-\Delta H_{1:1}$ (cor)[a]	$-\Delta H$ (E and C)[b]	$-\Delta H_{2:1}$ (cor)	$-\Delta H_T$ (cor)	$\Delta\nu_1$,[d] cm^{-1}	$\Delta\nu_2$,[d] cm^{-1}
CH_3CH	9.1	2.4	8.3	17.4	920	1820
C_5H_5N	16.1	11.7	12.1	28.2	1780	2190
N-Melm	16.4	16.4	10.5	26.9	1700	1900
piperidine	17.2	17.0	12.5	29.7	1780	1780
$(-CH_2CH_2)_2S$	15.0	14.0	10.3	25.3	1030	2110
caged phos	16.9	11.7	11.3	28.2	2200	5190
4-Pic-NO	9.0	9.1	6.4	15.4	210	1140
$(CH_3)_2SO$	10.6		6.5	17.1	1700	3120
C_6H_6		2.6				
CO					2200	
7-oxabicyclo[2.2.1]heptane		7.5			410	920

[a] Value obtained by adding -4.0 kcal mol^{-1} for benzene dissociation to the measured 1:1 enthalpy in Table I. [b] Using 1-methylimidazole, piperidine, and 4-picoline *N*-oxide: $E_A = -0.22$ ($\sigma = 0.2$), $C_A = 1.86$ ($\sigma = 0.03$). Essentially the same fit is obtained by using the extreme values for E_A and C_A (i.e., $\pm\sigma$). Thus, within experimental error $E_A = 0.0$, and $C_A = 1.83$; these values are used to calculate the enthalpy of 1:1 adduct formation. [c] This enthalpy has been corrected by -0.9 kcal mol^{-1} for the pyridine–benzene interaction.[13] [d] ν_0 for free Rh_2(butyrate)$_4$ is 6520 Å (15 340 cm^{-1}). $\Delta\nu_1 = \nu_{max(1:1)} - \nu_0$; $\Delta\nu_2 = \nu_{max(2:1)} - \nu_{0max(1:1)}$. The ν_{max} values are accurate to ± 40 cm^{-1}.

would be expected if the inductive effects of base coordination were effectively transmitted through the metal–metal bond to weaken the Lewis acidity of the second metal center. For solubility reasons, the thermodynamic measurements were carried out in benzene as the solvent. For most of the bases studied in this solvent, the enthalpy for coordinating the first base is about the same as that for coordinating the second. This is surprising in view of the three or four orders of magnitude decrease in K_2 compared to K_1. Since entropy effects this large could not be anticipated in the acid–base interaction, solvent participation is suspected. We propose a specific interaction between benzene and the rhodium butyrate dimer, forming a 2:1 adduct in pure benzene. When a strong base coordinates to $Rh_2(But)_4 \cdot 2C_6H_6$, the equilibrium

$$Rh_2(But)_4 \cdot B \cdot C_6H_6 \rightleftarrows Rh_2(But)_4 \cdot B + C_6H_6 \qquad (3)$$

lies well to the right; that is, nearly two benzenes are displaced when one base coordinates. This lowers the enthalpy measured for $\Delta H_{1:1}$ and increases $\Delta S_{1:1}$ from what one would obtain in the absence of benzene coordination. When the ΔH_T (i.e., $\Delta H_{1:1} + \Delta H_{2:1}$) value measured in benzene is compared with the solvation-corrected value from methylene chloride solutions for the pyridine adduct, a difference of ~ 4 kcal mol^{-1} results. The more negative enthalpy in methylene chloride solutions results because, in benzene solutions, solvent molecules must be displaced. Thus, coordination of two benzene molecules will have an enthalpy of coordination of about 4 kcal mol^{-1}, and addition of 3–4 kcal mol^{-1} to $-\Delta H_{1:1}$ (depending upon the position of the equilibrium in eq 3 for various bases) would make $-\Delta H_{1:1} > -\Delta H_{2:1}$ in all instances. The enthalpic as well as entropic contributions associated with benzene dissociation could give rise to the larger than statistical K_1 to K_2 ratio in benzene solutions. Variation in the position of the equilibrium in eq 3 resulting from base variations makes it difficult to interpret $\Delta H_{1:1}$ or $\Delta H_{2:1}$ values measured in benzene to within ± 0.8 kcal mol^{-1}. This complication is absent in the interpretation of ΔH_T because the benzene-solvated rhodium dimer is a constant species for all bases studied, and both benzenes are displaced in the process corresponding to 2:1 adduct formation. For the purpose of comparison, we have solvent corrected the enthalpies for 1:1 adduct formation by assuming that there is no benzene coordination in the 1:1 adduct. We might expect an overestimate of 1.5 kcal mol^{-1} as the maximum error that could arise in some of these adduct enthalpies. The 2:1 adduct enthalpy would then be underestimated by this amount.

In the course of 1:1 and 2:1 adduct formation, the visible absorption band at 15 337 cm^{-1} undergoes a shift to higher wavenumber. The shifts for the 1:1 and 2:1 adducts are presented in Table II as $\Delta\nu_1$ and $\Delta\nu_2$, respectively. A σ bonding interaction is expected to raise the energy of σ^* (see Figure 3) and cause a blue shift. If π back-bonding exists in addition to σ bonding, the π^* orbital will be stabilized, and this will also increase $\Delta\nu$. The large shift observed for the caged phosphite adduct suggests an extensive π-backbonding interaction; such an interaction influences the $\Delta\nu$ value to a greater extent than the enthalpy of adduct formation. Comparison of the shift for CH_3CN ($-\Delta H = 9.1$ kcal mol^{-1}) with that of 4-picoline *N*-oxide ($-\Delta H = 9.0$ kcal mol^{-1}) suggests π stabilization in the CH_3CN adduct. π back-bonding is also suggested in the pyr-

idine adduct for which the $\Delta\nu_1$ is comparable to that observed for piperidine, and greater than that of 1-methylimidazole, yet the enthalpy of pyridine adduct formation is significantly less than that of piperidine, and about the same for the 1-methylimidazole adduct. The electrochemical data also suggest significant π back-bonding in these adducts (vide infra). The sulfur atom of dimethyl sulfoxide is coordinated to the rhodium as indicated by an increase in S–O stretching frequency of this donor in the adduct.[21] Comparison of the enthalpies of adduct formation of this donor and tetrahydrothiophene with the $\pi^* \rightarrow \sigma^*$ frequency shifts of these adducts ($\Delta\nu_1$ or $\Delta\nu_2$ of Table II) indicate π back-bonding in the sulfoxide adduct. The electronegative oxygen is expected to lower the d-orbital energies of the sulfur atom in sulfoxide and provide a better energy match for the π-back-bonding interaction in the sulfoxide than in the sulfide.

Further support for π back-bonding in the 1:1 acetonitrile adduct comes from the infrared stretching frequency of the C≡N bond at 2265 cm^{-1}. It has been shown[22] that in σ-bond formation this band is expected to increase in frequency upon adduct formation, yet it asymmetrically broadens at lower frequency when rhodium butyrate is added to a solution of this donor. (A best estimate of the adduct stretching frequency is 2258 cm^{-1}.) This is attributed to an increase of electron density in the C≡N π^* orbital arising from a back-bonding interaction with rhodium, decreasing the force constant.

In order to further test the importance of the π-back-bonding abilities of this dimeric metal system, carbon monoxide was bubbled through a CH_2Cl_2 solution ca. 10^{-3} M in rhodium butyrate. Within about 10 s, the green solution had turned completely pinkish-purple, indicative of (presumably 2:1) adduct formation. The C–O infrared stretching frequency, ν_{CO} 2095 cm^{-1}, occurs at a lower energy than free CO (ν_{CO} 2143 cm^{-1}). This was reversible through an indefinite number of cycles by alternately bubbling CO and N_2 through the solution. The large $\Delta\nu_1$ and $\Delta\nu_2$ values (Table II) for the $\pi^* \rightarrow \sigma^*$ transition are consistent with extensive π stabilization of this adduct.

C. *E* and *C* Interpretation of the Data. The *E* and *C* model can be used to interpret and predict the σ-bonding interactions of Lewis acid–base adducts. The application of this equation to the interpretation of this data set is complicated by the extensive π-back-bonding ability of this rhodium dimer. Of the donors studied, we have presented evidence for the existence of this effect in CH_3CN, C_5H_5N, caged phosphite, $(CH_3)_2SO$, and CO. Though π back-bonding is greater in $(CH_3)_2SO$ than THTP, we cannot confidently state that π stabilization is absent in THTP. This leaves 1-methylimidazole, piperidine and 4-Pic-NO as donors that could be used in an *E* and *C* fit of the solution-corrected data for the 1:1 adducts. With potential errors in the solvent-corrected data from benzene coordination, the values of 0.0 and 1.8 (see Table II) for E_A and C_A are tentatively suggested for this acid.[23] "σ-only" enthalpies are then calculated for all of the donors of Table I using eq 1, and are listed in the column $-\Delta H$ (*E* and *C*) of Table II. Errors of ±0.8 kcal mol^{-1} are anticipated in the fit in view of the approximation made that both benzene molecules are dissociated when the 1:1 adduct forms. The measured $-\Delta H°_{1:1}$ for all donors that were not used to calculate E_A and C_A (with the exception of tetrahydrothiophene) are all much larger than the enthalpy predicted for a σ-type interaction. If we attribute the extra stabilization to π back-bonding (π stabilization plus synergism in the σ bond), π stabilization of 5–6 kcal mol^{-1} exists in the CH_3CN, caged phosphite, and pyridine adducts.

The benzene–rhodium dimer interaction is predicted to be 2.5 kcal mol^{-1} for the 1:1 adduct from the E_B (0.11) and C_B (1.4) values of benzene.[24] This value is consistent with a ~4.0 kcal mol^{-1} interaction of the dimer with two benzene molecules, since the enthalpy of coordination of the second benzene is expected to be less than that of the first.

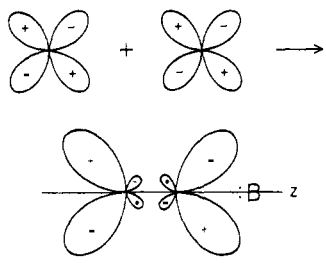

Figure 5. Rhodium d_{xz} (or d_{yz}) orbitals can combine to form the corresponding π^* orbitals, which are capable of undergoing π back-bonding to B.

The question that immediately arises is why π stabilization should be so much more important in this dimeric rhodium(II) system than in the reported rhodium(I) systems[25,26] where excellent *E* and *C* fits were obtained for the monomeric pyridine and CH_3CN adducts, indicating no π stabilization. The difference arises from what we feel will be a very important property of metal–metal bonding systems. The extensive overlap of d orbitals on the two metal centers gives rise to spatial characteristics for the π and π^* orbitals that make the chemistry of these systems unusual. In the case of the rhodium system, we focus on the filled π^* orbitals. As is illustrated in Figure 5, the combination of d_{xz} or d_{yz} orbitals gives rise to an antibonding orbital lobe that projects out toward an incoming donor ligand on the *z* axis (the donor is indicated by the symbol B in Figure 5). As indicated in Figure 3, these orbitals are populated in the rhodium system. The nature of these antibonding orbitals coupled with the fact that the butyrate ligands are essentially σ donors concentrates electron density in these antibonding orbitals and makes this rhodium(II) metal center very effective at undergoing a π-back-bonding stabilization. For example, this is the first metal complex in which excess stabilization for a pyridine ligand has been detected. Normal σ-type coordination accompanied by chloride bridge cleavage was observed not only with this donor, but also with CH_3CN toward the tetracarbonylrhodium(I) chloride dimer, the biscyclooctadienerhodium(I) chloride dimer, and the π-allylpalladium chloride dimer.[27]

D. Electrochemical Studies. Subsequent to our studies, Das, Kadish, and Bear[28] have reported the electrochemical behavior of a series of rhodium(II) carboxylates as a function of R-group and base variation of the 1:1 and 2:1 adducts of different bases in the same solvent. The results of our electrochemical studies on the 1:1 and 2:1 adducts of rhodium butyrate are summarized in Table III. The stabilization of the base coordinated to the cation relative to the base coordinated to the neutral dirhodium(II) butyrate can be obtained by combining the equations

$$e^- + Rh_2(butyrate)_4^+ \rightarrow Rh_2(butyrate)_4 \quad (4)$$

$$Rh_2(butyrate)_4B \rightarrow Rh_2(butyrate)_4B^+ + e^- \quad (5)$$

$$Rh_2(butyrate)_4B + Rh_2(butyrate)_4^+ \rightarrow Rh_2(butyrate)_4 + Rh_2(butyrate)_4B^+ \quad (6)$$

The free energies for this reaction are listed for the various bases involved in Table III as $-\Delta G(1:1)$. The 2:1 cationic species can be compared relative to the 1:1 species by combining the equations

$$e^- + Rh_2(butyrate)_4B^+ \rightarrow Rh_2(butyrate)_4B \quad (7)$$

$$Rh_2(butyrate)_4B_2 \rightarrow Rh_2(butyrate)_4B_2^+ + e^- \quad (8)$$

$$Rh_2(butyrate)_4B_2 + Rh_2(butyrate)_4B^+ \rightarrow Rh_2(butyrate)_4B + Rh_2(butyrate)_4B_2^+ \quad (9)$$

Table III. Reduction Potentials for $Rh_2(butyrate)_4B^+$ and $Rh_2(butyrate)_4B_2^+$ and the Free Energies Corresponding to Equations 6 and 9 for Various Base Adducts of $Rh_2(butyrate)_4$

base, B	$E_{1/2}(1:1)^a$	$E_{1/2}(2:1)^a$	$-\Delta G(1:1)^b$	$-\Delta G(2:1)^c$
CH_3CN	1.59	1.54	0.9	1.1
C_5H_5N	1.45	1.20	4.2	5.8
N-MeIm	1.37	1.04	6.0	7.8
piperidine	1.35	1.02[d]	6.5	7.6
$[-CH_2CH_2]_2S$	1.47[f]	1.28	3.7	4.4
caged phos	1.62	1.63	0.2	−0.2
4-Pic-NO	1.3		7.6	
$(CH_3)_2SO$	1.40	1.31[e]	5.3	2.0

[a] In volts vs. Ag^+/Ag. Ferrocene $E_{1/2} = 0.76$ and rhodium butyrate $E_{1/2} = 1.63$. [b] ΔG (kcal mol^{-1}) for the reaction in eq 6. [c] ΔG (kcal mol^{-1}) for the reaction in eq 9. [d] An estimate. This wave was irreversible. [e] An estimate. K_2 was not large enough to permit conversion of all the 1:1 adduct to 2:1 at reasonable base concentrations. The remaining 1:1 caused a distortion in the 2:1 wave. [f] An estimate. A discrete wave corresponding to a 1:1 adduct could not be detected. This is the potential observed for a solution containing equimolar amounts of $Rh_2(But)_4$ and THTP.

As the metal–ligand σ bond strength increases, the metal orbital nonbonding electrons are driven higher in energy and the adduct is more readily oxidized. The nature of the metal–ligand interaction in the cation (that is, its C/E ratio) is expected to differ from that of the neutral rhodium dimer, so a linear relation of neutral adduct σ bond strength vs. $E_{(1/2)}$ is not expected. The $E_{(1/2)}$ (1:1) should be lowered by an increase in the σ bond strength, and ΔG for eq 6 should become more negative. The same trends should be observed for $E_{(1/2)}$ (2:1) and $\Delta G(2:1)$. On the other hand, a π-back-bonding interaction should stabilize the metal π^* orbitals and increase $E_{(1/2)}(1:1)$ and $E_{(1/2)}(2:1)$, while $\Delta G(1:1)$ and $\Delta G(2:1)$ become less negative. This is equivalent to stating that the cation will be less effective at π back-bonding than the neutral acids. The important conclusion is that σ bonding and π back-bonding work in the same direction in contributing to the neutral adduct enthalpies, but in opposite directions in influencing $-\Delta G(1:1)$ and $-\Delta G(2:1)$. Thus, the combined experiments are diagnostic of the effect.

The adducts of piperidine, *N*-methylimidazole, and 4-picoline *N*-oxide are stabilized by 6–7 kcal on oxidation. These bases were used in the E and C fit of the calorimetry data as the standard σ donors. Even though the solvation-corrected enthalpy of adduct formation of the neutral dimer with pyridine (Table III) is greater than that of 4-picoline *N*-oxide, comparable to that of *N*-methylimidazole, and larger than the E and C prediction, the $-\Delta G(1:1)$ value is considerably smaller. This is the type of behavior expected from adducts in which π back-bonding is significant. In the neutral adduct E and C enthalpy interpretation, we previously claimed substantial π-back-bonding stabilization in the adducts of the CH_3CN, $(CH_3)_2SO$, and phosphite donors. In all instances the $\Delta G(1:1)$ values indicate significantly less stabilization of the cationic adducts of these bases than one observes for σ-donor bases. This behavior by π-acceptor bases provides strong support for the existence of substantial bond stabilization in the adducts from π back-bonding with tetra-μ-butyrato-dirhodium(II). The electrochemical potential of the CO adduct was 1.76 V, compared to 1.63 V for the free acid; this is the largest potential measured in this study. Since CO is widely accepted as a strong π acid and weak σ donor, this result is in complete accord with the interpretation presented here. (The oxidized adduct has lost an electron involved in π back-bonding and is less stable than the neutral adduct.)

The $\Delta G(2:1)$ values indicate the preference of the second coordinated base for the cationic acid compared to the neutral one. They are more difficult to interpret because the first base coordinated to the cationic acid changes each time. The $\Delta G(2:1)$ value, however, does indicate that the phosphite ligand prefers to coordinate to the neutral acid instead of the cation. This preference exists even though the cation is a better acceptor than the neutral acid toward σ donors. Hence, the $\Delta G(2:1)$ indicates extensive π stabilization for the second phosphite in the neutral acid, and that the π-back-bonding tendencies of the metal dimer are not satisfied by the coordination of just one phosphite.

Concluding Remarks

As mentioned earlier, the metal–metal interaction in the rhodium dimer concentrates an enormous amount of $d\pi^*$ electron density in the metal–ligand bonding region. This phenomenon can be likened to the trans effect. In the metal–metal system, the "trans ligand" is the other rhodium, and this second metal is extremely effective in pushing π^* density toward the incoming ligand. This realization suggests one very important way in which one metal in a molecule can influence the behavior of the second. The conclusion can be stated with the following generalization for metal–metal bonded systems: *the σ, π, or δ basicity of a transition metal ion in a given oxidation state is maximized if that ion is present as a d^8–d^8, d^7–d^7, or d^5–d^5 dimer, in which σ^*, π^*, or δ^* is the highest occupied molecular orbital, respectively. Similarly, the σ, π, or δ acidity is maximized in a d^0–d^0, d^1–d^1, or d^3–d^3 dimer, in which σ, π, or δ is the lowest unoccupied molecular orbital, respectively.* This conclusion relies on the maintenance of the MO ordering depicted in Figure 3 and a low spin disposition of electrons, an assumption that appears to be valid in the vast majority of neutral homonuclear dimers.[29]

An application of this principle may be made to a system which was reported by Gray and co-workers:[30] $Rh_2(bridge)_4^{2+}$ (where bridge = 1,3-diisocyanopropane). This Rh(I) dimer is d^8–d^8, and thus should be an optimum σ base, and ready protonation of this complex in aqueous acid is proposed. These authors prefer to think of this step as an acid–base reaction rather than oxidative addition (on the basis of spectroscopic evidence and ease of titration).

Acknowledgments. The authors acknowledge the generous support of this research by the National Science Foundation through Grant CHE 78-11553. We also acknowledge a generous loan of rhodium trichloride from Engelhard Industries.

Supplementary Material Available: All raw data used in the calculation of equilibrium constants and enthalpies (13 pages). Ordering information is given on any current masthead page.

References and Notes

(1) G. L. Eichhorn, Ed., "Inorganic Biochemistry", American Elsevier, New York, 1973.
(2) E. I. Solomon et al., *J. Am. Chem. Soc.*, **98**, 1029 (1976).
(3) R. A. Sheldon and J. K. Kochi, "Mechanisms of Metal-Catalyzed Oxidation of Organic Compounds in the Liquid Phase", **5**, 135 (1973).
(4) F. A. Cotton, *Chem. Soc. Rev.*, **4**, 27 (1975).
(5) F. A. Cotton et al., *Acta Crystallogr., Sect. B*, **27**, 1664 (1971).
(6) S. A. Johnson, H. R. Hunt, and H. M. Neumann, *Inorg. Chem.*, **2**, 960 (1963).
(7) J. Kitchens and J. L. Bear, *J. Inorg. Nucl. Chem.*, **32**, 49 (1970).
(8) M. J. Bennett, K. G. Caulton, and F. A. Cotton, *Inorg. Chem.*, **8**, 1 (1969).
(9) L. Dubicki and R. L. Martin, *Inorg. Chem.*, **9**, 673 (1970).
(10) J. G. Norman and H. J. Kolari, *J. Am. Chem. Soc.*, **100**, 791 (1978), and references cited therein.
(11) R. M. Richman, T. C. Kuechler, S. P. Tanner, and R. S. Drago, *J. Am. Chem. Soc.*, **99**, 1055 (1977).
(12) C. R. Wilson and H. Taube, *Inorg. Chem.*, **14**, 2276 (1975).
(13) R. S. Drago, *Struct. Bonding (Berlin)*, **15**, 73 (1973).
(14) T. O. Maier and R. S. Drago, *Inorg. Chem.*, **11**, 1861 (1972).
(15) P. Legzdins, R. W. Mitchell, G. L. Rempel, J. D. Ruddick, and G. Wilkinson, *J. Chem. Soc.*, 3322 (1970).
(16) F. A. Cotton and J. G. Norman, Jr., *J. Coord. Chem.*, **1**, 161 (1971).

(17) M. P. Li, Ph.D. Thesis, University of Illinois, 1976.
(18) R. S. Drago, N. O'Brien, and G. C. Vogel, *J. Am. Chem. Soc.*, **92**, 3926 (1970).
(19) F. Rohrscheid, A. L. Balch, and R. H. Holm, *Inorg. Chem.*, **5**, 1542 (1966).
(20) R. N. Adams, "Electrochemistry at Solid Electrodes", Marcel Dekker, New York, 1969, p 206.
(21) R. S. Drago and D. W. Meek, *J. Phys. Chem.*, **65**, 1446 (1961), and references cited therein.
(22) K. F. Purcell and R. S. Drago, *J. Am. Chem. Soc.*, **88**, 919 (1966).
(23) The information content of the enthalpies alone is low because an equally good fit could be obtained for pyridine, piperidine, *N*-methylimidazole, and acetonitrile. The electrochemistry and spectral data results are difficult to interpret on the basis of the fit involving these four bases.
(24) R. S. Drago, L. B. Parr, and C. S. Chamberlain, *J. Am. Chem. Soc.*, **99**, 3203 (1977).
(25) A. J. Pribula and R. S. Drago, *J. Am. Chem. Soc.*, **98**, 2784 (1976).
(26) M. P. Li and R. S. Drago, *J. Am. Chem. Soc.*, **98**, 5129 (1976).
(27) M. P. Li, R. S. Drago, and A. J. Pribula, *J. Am. Chem. Soc.*, **99**, 6900 (1977).
(28) K. Das, K. M. Kadish, and J. L. Bear, *Inorg. Chem.*, 17, 930 (1978).
(29) F. A. Cotton, *Acc. Chem. Res.*, **11**, 225 (1978).
(30) N. S. Lewis, K. R. Mann, J. G. Gordon II, and H. B. Gray, *J. Am. Chem. Soc.*, **98**, 7461 (1976).

A Novel Bimetallic Sulfur Cluster. Crystal and Molecular Structure of a Dimer of Bis[methyldiphenylphosphinesilver]tetrathiotungsten, $[(C_6H_5)_2PCH_3]_4Ag_4W_2S_8$

Judith K. Stalick,* Allen R. Siedle,*[1] Alan D. Mighell, and Camden R. Hubbard

Contribution from the Center for Materials Science, National Bureau of Standards, Washington, D.C. 20234. *Received November 14, 1978*

Abstract: The title compound, I, is formed from $[(C_6H_5)_2PCH_3]_4Ag_2WS_4$ (II) with loss of phosphine in polar solvents. The crystal and molecular structure of I has been determined from three-dimensional X-ray data collected by counter methods. The molecular compound I crystallizes in the monoclinic space group $P2_1/n$ with $Z = 2$ and cell dimensions $a = 11.901$ (4) Å, $b = 12.233$ (5) Å, $c = 20.375$ (10) Å, $\beta = 92.25$ (3)°. The observed and calculated densities are 2.04 and 2.08 g/cm^3, respectively. The structure has been refined to a final R factor on F of 0.049 for 2096 observed reflections. The structure of I consists of a 12-atom cluster containing four silver atoms, two tungsten atoms, and six sulfur atoms; the cluster possesses a crystallographic center of symmetry. Based on ^{31}P NMR data for II and the structures of the closely related $[(C_6H_5)_2PCH_3]_2Au_2MS_4$ compounds (M = Mo, W), a mechanism for the formation of I from II is proposed.

Introduction

The chemistry of molecular metal sulfides is currently a subject of much interest. Iron–sulfur aggregates, in particular, have been closely studied because of analogies to biological electron-transfer components.[2-4] Sulfur-bridged molybdenum compounds have been scrutinized in order to learn about the role of this group 6B metal in nitrogen fixation[5] and in redox-active molybdoenzymes such as xanthine, aldehyde and sulfite oxidases, and nitrate reductase.[6,7]

Following the development of a general synthesis for bimetallic sulfur arrays of the type $L_nM_2M'S_4$ (L = tertiary phosphine; M = Cu, Ag, Au; M' = Mo, W),[8] systematic X-ray crystallographic studies have been carried out to obtain further insight into the structure and bonding of these materials. This paper reports the crystal and molecular structure of $[(C_6H_5)_2PCH_3]_4Ag_4W_2S_8$, a novel bimetallic sulfur cluster with surprisingly different architecture from that of the stoichiometric gold analogue, $[(C_6H_5)_2PCH_3]_2Au_2WS_4$.[8]

Experimental Section

Preparation of $[(C_6H_5)_2PCH_3]_4Ag_4W_2S_8$ (I). $[(C_6H_5)_2PCH_3]_4Ag_2WS_4$ (II) was prepared as previously described.[8] A solution of 0.58 g (4.4 mmol) of II in 50 mL of 1:1 acetone–1,2-dichloroethane was degassed by two freeze–pump–thaw cycles and allowed to stand at room temperature. After 7 days 0.11 g (22%) of crystalline I had separated. The crystals were washed with a small amount of 1,2-dichloroethane and vacuum dried. Anal. Calcd: C, 33.62; H, 2.80; Ag, 23.27; P, 6.68; S, 13.79; W, 19.83. Found: C, 33.64; H, 2.82; Ag, 23.24; P, 6.67; S, 13.81; W, 19.81. Recrystallization from acetonitrile yielded small, orange crystals suitable for X-ray analysis.

Unit Cell and Space Group. Precession photographs of the $h0l$, $h1l$, and $0kl$ zones indicated monoclinic symmetry with systematic absences $0k0$, $k \neq 2n$, and $h0l$, $h + l \neq 2n$, uniquely establishing space group C_{2h}^5-$P2_1/n$ [equivalent positions: $\pm(x, y, z)$; $\pm(\frac{1}{2} + x, \frac{1}{2} - y, \frac{1}{2} + z)$]. The cell dimensions, obtained using Mo Kα radiation ($\lambda = 0.7107$ Å) by centering 15 reflections on an automated diffractometer, are $a = 11.904$ (4) Å, $b = 12.233$ (5) Å, $c = 20.375$ (10) Å, $\beta = 92.25$ (3)°. The observed density of 2.04 g/cm^3 obtained by flotation agrees with the calculated value of 2.080 g/cm^3 assuming $Z = 2$ on the basis of the dimeric structure subsequently determined. A crystallographic center of symmetry thus is imposed upon the metal cluster I.

Collection and Reduction of the Intensity Data. A small crystal of approximate dimensions 0.05 × 0.06 × 0.08 mm was mounted parallel to the [100] direction. Diffractometer data were obtained using graphite-monochromated Mo Kα radiation by the bisecting mode, θ–2θ scan technique. The peaks were scanned from 1.0° on the low-angle side of the Kα_1 peak to 1.1° on the high-angle side of the Kα_2 peak using a variable scan rate; background counts were taken at each end of the scan with the ratio of total background time/scan time = 1.0.

A unique data set was collected to $2\theta = 40°$. Three reflections, monitored periodically, showed no significant change in intensity during data collection. The intensities were corrected for background, and standard deviations were assigned according to the equation $\sigma(I) = [I + (KI)^2]^{1/2}$, where the value of 0.017 13 used for K was obtained from a statistical analysis of the intensity distributions of the three standard reflections.[9] The data were also corrected for Lorentz and polarization effects. Because the crystal faces were poorly defined and the absorption coefficient was 59.2 cm^{-1}, no absorption correction was applied. Transmission coefficients ranged from 0.62 to 0.74. Of the 2786 unique data collected, 2096 reflections were considered to be observed with $I \geq 3\sigma(I)$, although all data were used in the final structure refinement.

Solution and Refinement of the Structure. Conventional Patterson and Fourier techniques readily yielded the positions of all nonhydrogen